

---

## Source term determination for sabotage against casks with vitrified high level waste

*W. Brücher\*, R. Martens\*, G. Pretzsch\*, O. Nolte\*\*, W. Koch\*\*, A. Holzwarth\*\*\**

\*Gesellschaft für Anlagen- und Reaktorsicherheit GRS mbH, Schwertnergasse 1, 50667 Köln, Germany

\*\*Fraunhofer-Institut für Toxikologie u. Experimentelle Medizin, Nikolai-Fuchs-Str. 1, 30625 Hannover, Germany

\*\*\* Fraunhofer-Institut für Kurzzeitdynamik, Am Klingenberg 1, 79588 Efringen-Kirchen, Germany

---

### Abstract:

A sabotage attack with a conical shaped charge (CSC) to a transport and storage cask containing vitrified high-level waste (HLW) could result in the generation of particulate radioactive matter from fractured glass in the cask interior and subsequently to an airborne release to the environment. This potential airborne source term has to be known for the assessment of radiological consequences. Source term determination for HLW so far was based on scaled experiments performed at Battelle, which had some limitations and uncertainties. A series of small and real scale experiments on the effect of a CSC impact onto non radioactive but chemically equivalent vitrified HLW mock-ups was performed in order to quantify the airborne release from the samples and from a surrounding cask. Special focus of the experiments was on the scalability of results, on the volatile element enhancement in the respirable aerosol fraction and on the release process. Resulting particle size distributions as well as volatile element enhancement data are comparable for all scales. The maximum particle release from real scale experiments is in good agreement with earlier estimates but observed enhancement factors are significantly lower. Thus, calculated potential radiological consequences are yet lower than previously assumed.

## 1 INTRODUCTION

A sabotage attack with a conical shaped charge (CSC) to a transport and storage cask containing vitrified high-level waste (HLW) could result in the generation of particulate radioactive matter from fractured glass in the cask interior and subsequently to an airborne release to the environment. This potential airborne source term is a prerequisite for the assessment of radiological consequences. Former assessment of the potential source term from vitrified HLW transport and storage casks were based on experiments with radioactive and non-radioactive small scale glass samples performed in the eighties at Battelle Columbus, Ohio. However, due to the reduced scale, the scatter of results and the limited resolution of the relevant particle size range in the hot experiments the according source term estimation contains some unsatisfactory degree of uncertainty. Later HLW surrogate glass experiments at Battelle had a wider sampling range but only depleted uranium as a tracer [1].

Other real scale and small scale experiments in the USA and in Germany [2, 3, 4] were focussed on casks for spent fuel. Due to the different material properties and geometry of the inventory a simple transfer of these results to vitrified HLW is not possible. Therefore, a new set of small scale and real scale experiments was initiated in order to increase the accuracy of radiological consequence analyses of a CSC sabotage attack on vitrified HLW.

Processes affecting the source term to the environment are

- aerosol release inside the cask
- loss and screening processes (e.g. deposition)
- transfer processes (e.g. volatile element enhancement, see below)
- release to the environment

The formation of airborne non-volatile material is related to brittle fracture of the target material initiated by the metallic jet of the CSC remaining after penetration of the cask wall. For a radiological consequence analysis two exposure pathways are of interest: inhalation and ground shine. Other pathways can be neglected due to their low contribution or due to mitigating measures. For inhalation only the respirable particles with an AED  $< 10 \mu\text{m}$  (aerodynamic equivalent diameter) are relevant, whereas coarse aerosol particles with an AED up to  $100 \mu\text{m}$  also contribute to the ground shine dose. However, a finer resolution of the particle size distribution (PSD) is necessary as many relevant processes of aerosol release and transport are size dependant. This especially holds for the effect of volatile element enhancement (or enrichment) in the small particle size range.

High level vitrified waste materials consist of non-volatile nuclides as well as fission products with high volatility such as caesium compounds, for example. Apart from fracture the high energy of the metallic CSC jet also generates high temperatures within the penetrated area. As a consequence isotopes of volatile elements can evaporate and re-condense to the aerosol cloud again. This leads to an enhancement of the content of volatile elements the fine airborne particles compared to the mass fraction of the same element in the bulk material. The relevant quantity for consequence analyses is the cumulative mass fraction of chemical element in the respirable size range compared to the mass fraction in the bulk material. This ratio is called integrated enhancement factor (IEF). Experiments with radioactive and non-radioactive small scale glass samples performed in the early eighties at Battelle Columbus suggested a conservative estimate of approximately 50 for the respirable range caesium IEF. However, this number was based on measured particle size distributions up to  $4 \mu\text{m}$  AED from small scale samples.

Due to the localized damage to the cask by a CSC and due to aerosol loss processes inside only a small fraction of aerosol generated inside the cask will be released to the environment. Therefore, it is important to quantify this release fraction in order to avoid unrealistic estimates of the source term which could result in excessive instead of adequate safety measures. Based on the small scale experiments performed by Battelle the upper estimate of aerosol release in the respirable size range from a real scale cask was in the order of magnitude of a gram, which is similar to experiments for spent fuel surrogate [2]. Due to the scatter of the Battelle data (one order of magnitude) and due to the limited knowledge about the relevant release mechanisms and about the transferability of reduced scale data to real scale it became evident that more insight into the release process was needed. This would enable a reliable transfer of experimental results to real scale and boundary conditions. Hence, a new set of small scale and large scale experiments was initiated to increase the accuracy of future source term determination and radiological consequence analyses. Major fields of interest in this experimental programme were

- the scalability of results
- the volatile element enhancement
- the release process.

## 2 EXPERIMENT SETUP

### 2.1 Test Specimen and CSC

We used vitrified waste simulant and experimental setups allowing for interaction of CSC jets of different calibres with surrogate targets of different shapes and sizes and simultaneous size selective sampling of the released aerosol. The test samples were fabricated at the Karlsruhe Research Centre during the non-radioactive test operation of a vitrification pilot plant for high-level waste. The material was composed of about 84 wt.% of a borosilicate glass matrix. The remaining 16 wt.% consisted of non-radioactive elements or chemically similar elements representing fission products, actinides and corrosion products. The non-volatile components were replaced by lanthanum (III) oxide and neodymium (III) oxide with melting point well above 2000 °C (see Table 1). A representative for the volatile compounds is caesium oxide with a melting point of 490°C. For the small scale tests we used cylindrical samples with a diameter between 14 and 204 mm and a height between 80 and 200 mm. Most samples were clad by a stainless steel mantle. For the large scale test original stainless steel canisters (Ø=430 mm, glass filling level ~ 1100 mm) for high-activity waste were used (Fig. 1).

**Tab. 1:** Relevant components of the non-radioactive high-level waste (HLW)

Compound	Weight percent [%]	Melting temperature [°C]
glass matrix: SiO <sub>2</sub> , MgO, CaO, Na <sub>2</sub> O..	84	-
HLW	16	-
Cs <sub>2</sub> O	0.44	490
La <sub>2</sub> O <sub>3</sub>	1.82	2000
Nd <sub>2</sub> O <sub>3</sub>	1.04	2320



**Fig. 1:** Clad small scale glass specimen (left), real scale glass canister with lifting unit (right)

The small scale tests were carried out with explosive charges fabricated at the explosive laboratory at the Fraunhofer Institut für Kurzzeitdynamik, Germany. For the full sized glass canisters a real scale CSC was used.

## 2.2 Small Scale Setup

The distribution of total mass released as well as relevant chemical elements were measured as a function of the aerodynamic particle diameter. Particle size distribution measurements were carried out using an apparatus in which a small calibre CSC interacted with a small scale target of vitrified waste simulant enabling

- in-situ separation between airborne particles and non-airborne fragments
- in-situ aerodynamic size classification of the airborne fraction

This apparatus (Fig. 2) consists of a vertical elutriation box separating the large debris from the airborne particles ( $<100\ \mu\text{m}$  AED) by suspending them in an upward directed homogeneous airflow. Larger particles settle on the bottom plate of the elutriator whereas the aerosol fraction passes a foam layer which retains fragments in the size range between 10 and  $100\ \mu\text{m}$  AED or is led to a coarse particle classifier collecting particles in three size intervals between 100 and  $21\ \mu\text{m}$ . Only particles with AED  $< 21\ \mu\text{m}$  are able to pass the  $180^\circ$  bend and are collected on a back-up filter. A side stream of this fraction is further classified by conventional Berner cascade impactors, covering the particle size range between 0.1 and  $10\ \mu\text{m}$  or 0.01 and  $21\ \mu\text{m}$ , respectively. In total, the measured aerosol size range extends over three orders of magnitude at least from 0.1 to  $100\ \mu\text{m}$  AED. For details of the apparatus see [5].

The CSC was placed inside of a cylindrical blast shield. Simultaneously with ignition of the CSC a shutter closes the connecting duct in order to minimize the disturbance of the air stream inside of vertical elutriator. After penetration of the vertically fixed specimen the CSC jet was captured by a steel stop block flanged to the elutriator box.

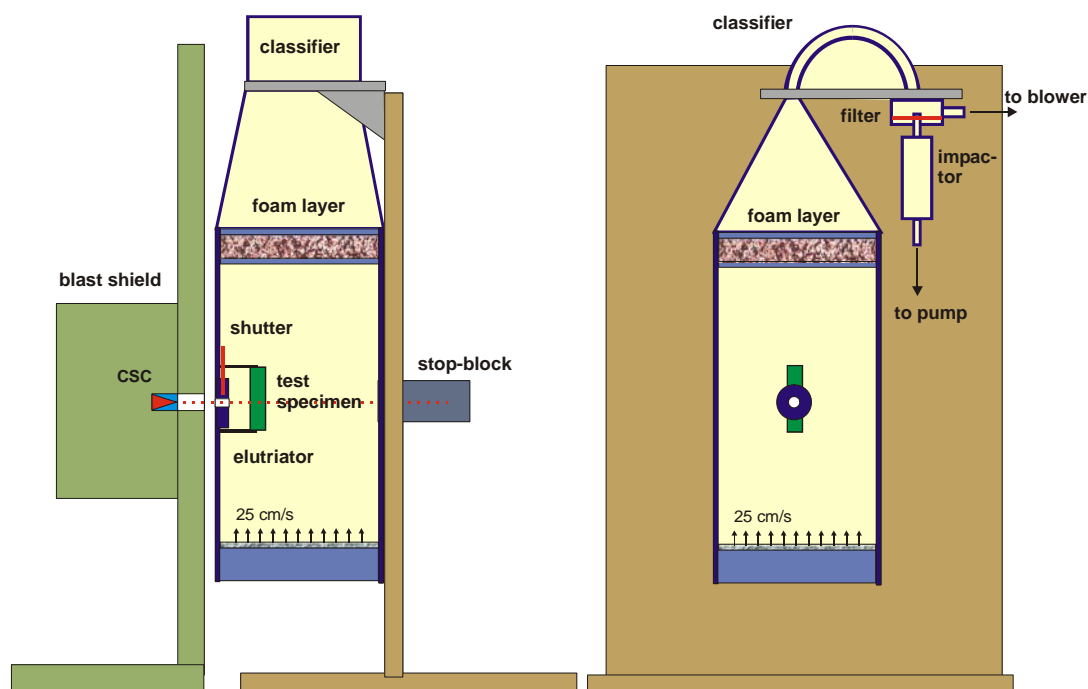


Fig. 2: Sketch of the small scale test setup

## 2.3 Real Scale Setup

The large scale tests were aimed to simulate a realistic accident scenario. A flexible transport cask model was designed in order to meet the following requirements:

- realistic cask geometry with regard to wall thickness and composition and free inner volume.
- possibility to measure the source term in- and outside the cask.

The transport cask model is an air-tight container made from reinforced concrete (Fig. 3). The top is sealed with a detachable steel lid. In the front wall a cylindrical steel duct can be equipped with representative cask wall specimen (disks) made from any desired cask wall material. The CSC is located behind a blast shield in order to prevent the aerosol equipment from damage. The CSC jet passes an aerosol sampling chamber (vertical elutriator) the cask wall elements and finally penetrates the glass canisters inside the test container. Potential remains of jet are caught with a stop block inside the test container.

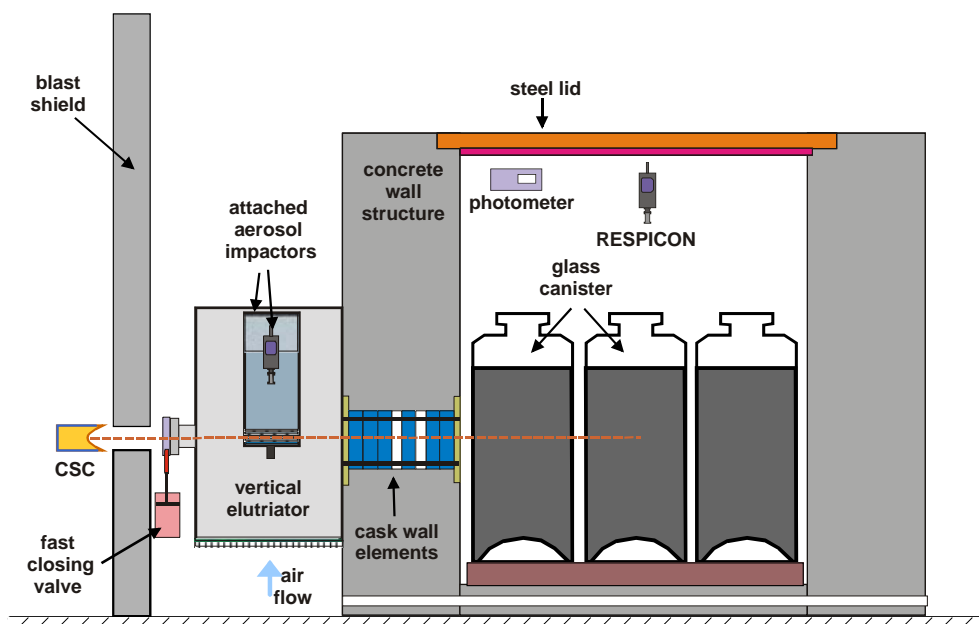


**Fig. 3:** Sketch of the real scale test setup

The sampling methods for the aerosol released from the container are similar to the small scale tests. An aerosol sampling chamber with a vertical elutriator is attached in front of the container wall in order to collect the total particulate/airborne release through the penetration channel. The entrance hole of the elutriator is closed by a fast closing valve simultaneously with the ignition of the charge. The entire airflow with aerosols  $< 100 \mu\text{m}$  AED passes through a 4-stage coarse particle impactor ( $100$  to  $< 5 \mu\text{m}$ ) which is attached to the vertical elutriator chamber. In parallel side stream sampling to additional particles impactors with 8 stages ( $16$  to  $0.06 \mu\text{m}$ ) and to a time resolved 3-stage aerosol spectrometer (Respicon™ [6], respirable, thoracic and inhalable fraction) is possible.

Inside the concrete container particle size distribution and the temporal concentration pattern were also sampled by a Marple Impactor, an aerosol photometer and a Respicon™. In addition to the aerosol measuring devices two fast response thermocouples and one fast response pressure gauge were installed inside the test container. The initial pressure of the cask atmosphere could be lowered to typical cask conditions.

### 3 RESULTS

The presentation of results will concentrate on four real scale tests with glass canisters which were carried out in a longer test series also including cement targets and on five small scale tests with clad glass specimen.

#### 3.1 Aerosol release

All shots were connected with an increase of the atmosphere temperature inside the test container. The real scale tests show a temperature rise which is correlated with the amount of released aerosol (Fig. 4). Due to the variation of the target geometry inside the real scale test container there was a significant variation in aerosol mass concentration within these tests. The temperature rise was caused either by heat transfer from hot particles generated by the jet impact or by the oxidation of hot iron particles originating from the target cladding or jet stop block. The latter mechanism can be precluded in real casks filled with helium.

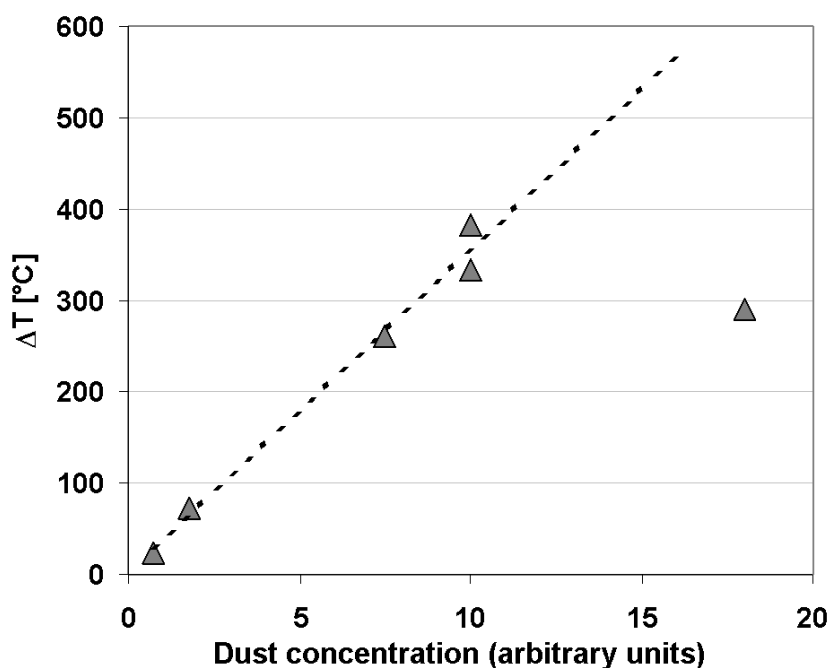


**Fig. 4:** Influence of dust concentration on temperature rise inside the test container (real scale tests, glass or cement targets, peak temperature derived from peak pressure)

From an analysis of pressure data a contribution of external gases to the cask atmosphere could be excluded. Depending on the temperature rise and on the initial cask atmosphere pressure in some experiments a short period of overpressure was observed forcing a blow-down of the cask atmosphere. Heat losses from the hot atmosphere to internal surfaces significantly damped the blow-down process. Therefore, even in tests with short-time overpressure only a small fraction of the inside aerosol was released to the aerosol sampling chamber attached to the front wall. The release fraction further decreased when no overpressure occurred.

### 3.2 Size distributions

Aerosol size distributions derived from glass CSC experiments typically show a similar shape as particle size distributions from lower speed impact experiments, e.g. with a light gas gun (Fig. 5). These linear shapes of cumulative particle size distributions in double logarithmic presentation are found for a wide range of specific energy impact of brittle material [6]. PSD shapes of small scale and real scale CSC experiments are comparable.

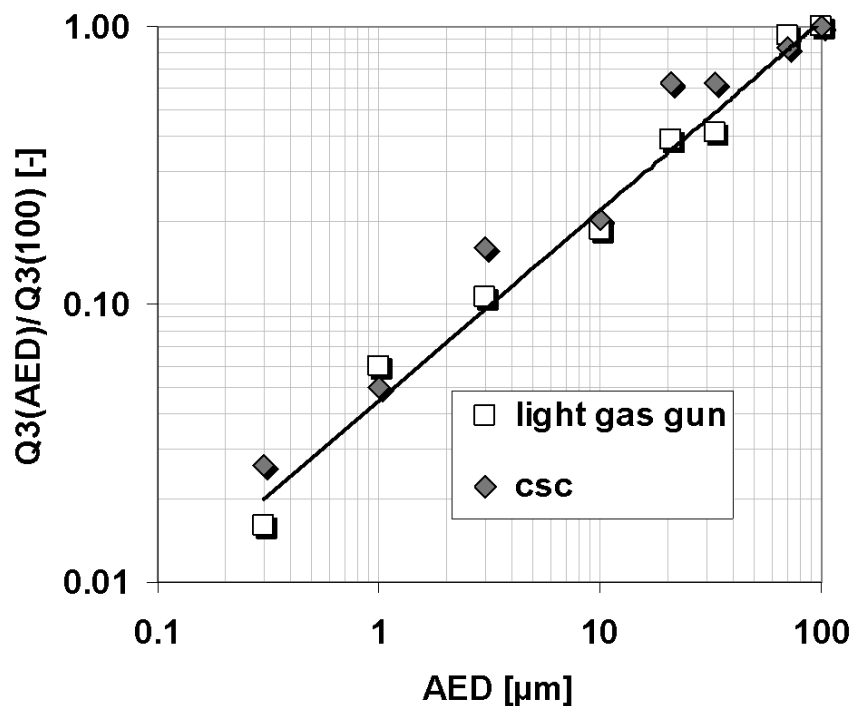


**Fig. 5:** Cumulative particle size distributions Q3 of brittle glass fracture from a CSC impact compared to a light gas gun shot (normalized to Q3 at 100  $\mu\text{m}$  AED)

Impactor and Respicon™ stages were chemically analyzed in order to separate contributions from different aerosol sources and to analyse variations within different chemical elements of the HLW surrogate glass. Within the respirable size range some interesting observations were made (Fig 6):

- The lowest particle size range  $< 1 \mu\text{m}$  is dominated by copper from the CSC inlay whereas glass (derived from lanthanum analysis) has no significant contribution to the total mass in this size range.
- Caesium and copper PSDs show a similar shape.
- The caesium to glass fraction (enhancement factor) increases with decreasing AED.

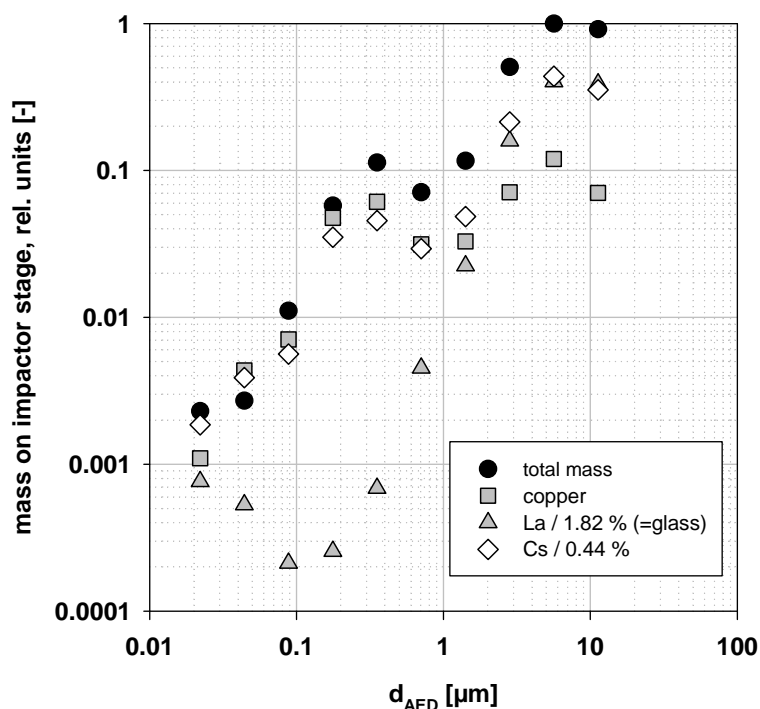


**Fig. 6:** Particle size distribution  $<math>< 10 \mu\text{m}</math> AED for copper, glass (as determined from lanthanum), caesium (normalized to its content in the bulk glass material) and the total mass measured with a 10 stage Berner impactor (Exp. No. s#2)$

Hence, there is a significant variation between chemical elements contributing to the respirable aerosol size range. The consequences for the volatile element enhancement are discussed in the following section.

### 3.3 Volatile element enhancement

The caesium mass transfer within the size distribution of aerosols is caused by evaporating caesium or caesium compounds from the hot region of jet impact and a subsequent recondensation as aerosols or on aerosols. The similar shape of the size distribution of copper and caesium (Fig. 6) suggests an interaction of evaporated copper and caesium in the AED size range below  $1 \mu\text{m}$ . As the recondensation mode of copper and caesium is more shifted to small aerosol diameters compared to the size distribution from brittle fracture of glass the differential enhancement factor (EF) for caesium increases with decreasing particle diameter (Fig. 7).

The size distributions of caesium enhancement in Fig. 7 show some differences between both experimental scales but the respective integrated enhancement factors for the whole respirable range (Tab. 2), which are more relevant for consequence assessment, are rather similar for both scales. This is due to the fact that most aerosol mass is within the larger particle size range with rather similar differential enhancement factors in both test scales. However, there seems to be a scaling effect for very small samples (s #1) relative to the CSC size where the sample diameter limits the volume of brittle glass fracture but not the (smaller) hot region of CSC jet impact where evaporation takes place. Hence, the integrated enhancement factor is highest for this sample.

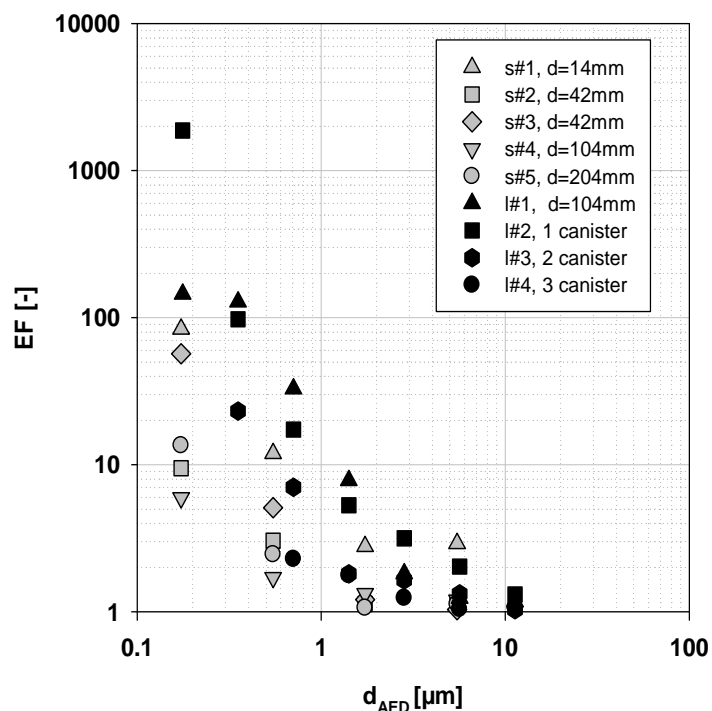


**Fig. 7:** Size dependence of the caesium enhancement factor for small scale tests in comparison to real large scale tests

**Tab. 2:** Small scale and real scale glass test matrix with integrated caesium enhancement factors for particles < 10 µm AED (IEF(10))

Exp. No.	Target	CSC	IEF(10)
s #1	cylinder, Ø14 mm	small scale	7.6
s #2	cylinder, Ø42 mm		1.7
s #3	cylinder, Ø42 mm		2.0
s #4	cylinder, Ø104 mm		2.2
s #5	cylinder Ø204 mm		1.7
l #1	cylinder, Ø104 mm	real scale	2.8
l #2	1 full sized canister		4.4
l #3	3 full sized canister		2.6
l #4	3 full sized canister		1.3

Integrated enhancement factors for caesium in the respirable size range all vary between 1.3 and 7.6 which is much lower than earlier predicted from the limited particle size distributions of the radioactive glass experiments by Battelle. The variation of IEF values may partly be attributed to the variation of target configuration and the variance in CSC performance. However, there seems to be an additional positive correlation of the IEF with the temperature of the cask atmosphere [Fig.8] which is plausible with respect to the supposed evaporation and recondensation mechanisms.

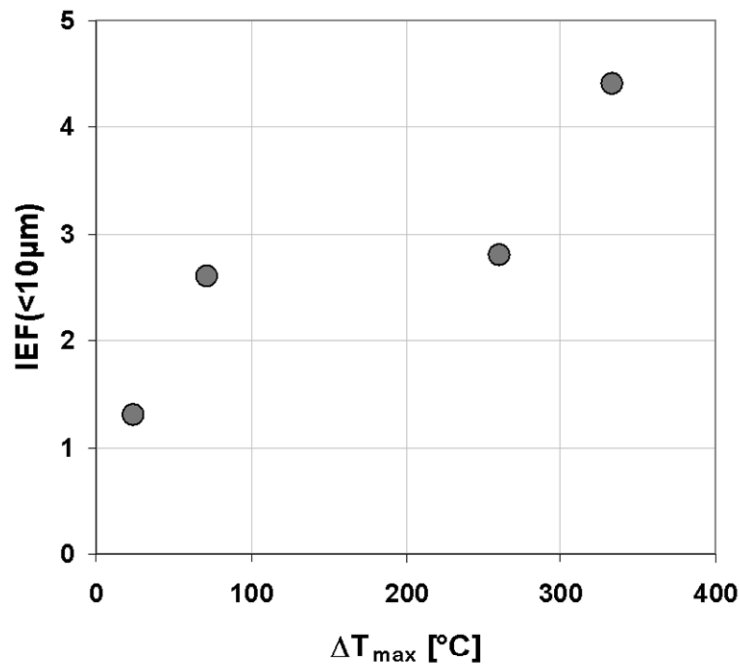


**Fig. 8:** Dependence of the integrated caesium enhancement factor on the temperature rise of the cask atmosphere (real scale tests)

## 4 CONCLUSIONS

The test series provided a much more detailed insight into the mechanisms of aerosol generation inside the cask and release processes to the environment compared to previous knowledge. Quantitative and qualitative data could be derived as a basis for an improved source term determination for a CSC sabotage attack against a transport and storage cask filled with vitrified HLW waste. For a further improvement and confirmation of results some additional tests on special topics e.g. the cause of the atmosphere temperature rise are necessary. The new experimental data as well as future experimental contributions will help to further develop and to validate source term models for sabotage consequence analyses.

Some results already allowed to refine current consequence analyses. The integrated caesium enhancement factor in the respirable range for vitrified HLW is significantly below the estimated factor derived from former Battelle experiments with hot samples which only resolved the small diameter part of the respirable aerosol range. These new results are supported by recent comparative glass tests in a different semi-open test apparatus at Sandia National Laboratories within an international sabotage test program on spent fuel release [4]. No significant influence of the experiment scale on integrated enhancement of volatile elements was found in our experiments as long as the target dimension does not limit the transverse extent of the brittle fracture volume. Therefore, a direct transfer of enhancement results from small scale experiments to real scale scenarios still appears to be adequate. The potential temperature effect on IEF values needs more investigation.

Maximum aerosol release data from these experiments are in good agreement with earlier upper estimates based on the small scale Battelle experiments. Due to the reduced enhancement factor potential radiological consequences of a sabotage attack against a HLW transport and storage cask are yet lower as previously assumed.

## 5 REFERENCES

1. Miller, N.E., A.W. Fentiman, M.R. Kuhlman, H.N. Ebersole, B.D. Trott, J.E. Orban: Radiological source terms resulting from sabotage to transport casks: Final report, NUREG/CR-4447, BMI-2131, Battelle Columbus, OH, November 1986.
2. Lange, F., G. Pretzsch, E. Hörmann, W. Koch: Experiments to quantify potential releases and consequences from sabotage attack on spent fuel casks. PATRAM 2001 Sep. 2-7, 2001, Chicago, IL.
3. Sandoval, R.P., J.P. Weber, H.S. Levine, A.D. Romig, J.D. Johnson, R.E. Luna, G.J. Newton, B.A. Wong, R.W. Marshall, Jr., J.L. Alvarez, and F. Gelbard: An assessment of the safety of spent fuel transportation in urban environs, SAND82-2365. Sandia National Laboratories, June 1983.
4. Molecke, M.A., J.E. Brockmann, L.A. Klennert, M. Steyskal, M.W. Gregson, W. Koch, O. Nolte, W. Brücher, G. Pretzsch, B. Autrusson and O. Loiseau: Spent fuel sabotage testing: Depleted uranium dioxide aerosol results, PATRAM 2007, Oct. 21-26, 2007, Miami, FL.
5. Mädler, L., W. Koch, F. Lange, K. Husemann: In-situ aerodynamic size classification of aerosols in the size range between 0.1 and 100  $\mu\text{m}$  for dustiness tests and powder characterization. *J. Aerosol Sci.*, 30, 451, 1999.
6. Lange F., R. Martens, E. Hörmann, W. Koch, O. Nolte, I. Gray, C. Ringot, N. Carr, L. van Velzen and S. Hughes: Improvement of the radiological and experimental basis to further develop the requirements of the IAEA transport regulations for LSA/SCO materials, a joint research study for CEC by GRS, Nirex, NRG, NRPB, 2003.